Adaptive Beamforming Assisted Receiver

Sheng Chen

Sheng Chen is with the School of Electronics and Computer Science, the University of Southampton, Southampton SO17 1BJ, U.K. E-mails: sqc@ecs.soton.ac.uk

Abstract

Adaptive beamforming is capable of separating user signals transmitted on the same carrier frequency, and thus provides a practical means of supporting multiusers in a space-division multiple-access scenario. Moreover, for the sake of further improving the achievable bandwidth efficiency, high-throughput quadrature amplitude modulation (QAM) schemes have becomes popular in numerous wireless network standards, notably, in the recent WiMax standard. This contribution focuses on the design of adaptive beamforming assisted detection for the employment in multiple-antenna aided multiuser systems that employ the high-order QAM signalling. Traditionally, the minimum mean square error (MMSE) design is regarded as the state-of-the-art for adaptive beamforming assisted receiver. However, the recent work [1] proposed a novel minimum symbol error rate (MSER) design for the beamforming assisted receiver, and it demonstrated that this MSER design provides significant performance enhancement, in terms of achievable symbol error rate, over the standard MMSE design. This MSER beamforming design is developed fully in this contribution. In particular, an adaptive implementation of the MSER beamforming solution, referred to as the least symbol error rate algorithm, is investigated in details. The proposed adaptive MSER beamforming scheme is evaluated in simulation, in comparison with the adaptive MMSE beamforming benchmark.

Index Terms

Smart antenna, adaptive beamforming, quadrature amplitude modulation, minimum symbol error rate, minimum mean square error, stochastic algorithm, least mean square algorithm, least symbol error rate algorithm

I. INTRODUCTION

The ever-increasing demand for mobile communication capacity has motivated the development of antenna array assisted spatial processing techniques [2]-[14] in order to further improve the achievable spectral efficiency. A specific technique that has shown real promise in achieving substantial capacity enhancements is the use of adaptive beamforming with antenna arrays [3],[10]. Through appropriately combining the signals received by the different elements of an antenna array, adaptive beamforming is capable of separating user signals transmitted on the same carrier frequency, provided that they are separated sufficiently in the angular or spatial domain. Adaptive beamforming technique thus provides a practical means of supporting multiusers in a space-division multiple-access scenario. For the sake of further improving the achievable bandwidth efficiency, high-throughput quadrature amplitude modulation (QAM) schemes [15]

have become popular in numerous wireless network standards. For example, the 16-QAM and 64-QAM schemes were adopted in the recent WiMax standard. Classically, the beamforming process is carried out by minimising the mean square error (MSE) between the desired output and the actual array output, and this principle is rooted in the traditional beamforming employed in sonar and radar systems. An advantage of this minimum MSE (MMSE) beamforming design is that its adaptive implementation can readily be achieved using the well-known least mean square (LMS) algorithm [16]-[21]. The MMSE design has been regarded as the state-of-the-art for adaptive beamforming assisted receiver, despite of the fact that, for a communication system, it is the bit error rate (BER) or symbol error rate (SER) that really matters.

Ideally, the system design should be based directly on minimising the BER or SER, rather than the MSE. Adaptive beamforming design based directly on minimising the system's BER has been proposed for the binary phase shift keying (BPSK) modulation [22]-[28] and quadrature phase shift keying (QPSK) modulation [29],[30]. These studies have demonstrated that the adaptive minimum BER (MBER) beamforming design can significantly improve the system performance, in terms of achievable BER, over the conventional MMSE design. The MBER beamforming is the true state-of-the-art and it is more intelligent than the MMSE solution, since it directly optimises the system's BER performance, rather than minimising the MSE, where the latter strategy often turns out to be deficient in the rank-deficient situation when the number of the users supported exceeds the number of the receiver antennas. Thus, the adaptive MBER beamforming design has a larger user capacity than its adaptive MMSE counterpart. Simulation results also show that the MBER design is more robust in near-far situations than the MMSE design. For the system that employs high-order QAM signalling, it is computationally more attractive by minimising the system's SER. This has led to the adaptive minimum SER (MSER) beamforming design for QAM systems [1]. The present constribution expands the work of [1] and provides a detailed investigation for the adaptive MSER beamforming design for the generic multiple-antenna assisted multiuser system employing high-order QAM signalling.

The organisation of this contribution is as follows. Section II introduces the system model, which is used in Section III for studying the adaptive MMSE and MSER beamforming designs. Section IV concentrates on investigating the achievable SER performance of the proposed adaptive MSER scheme in both the stationary and Rayleigh fading channels, using the adaptive MMSE scheme as a benchmark, while Section V presents the concluding remarks.

II. SYSTEM MODEL

The system supports S users, and each user transmits an M-QAM signal on the same carrier frequency of $\omega = 2\pi f$. For such a system, user separation can be achieved in the spatial or angular domain [12],[14] and the receiver is equipped with a linear antenna array consisting of L uniformly spaced elements. Assume that the channel is narrow-band which does not induce intersymbol interference. Then the symbol-rate received signal samples can be expressed as

$$x_l(k) = \sum_{i=1}^{S} A_i b_i(k) e^{j\omega t_l(\theta_i)} + n_l(k) = \bar{x}_l(k) + n_l(k), \tag{1}$$

for $1 \leq l \leq L$, where $t_l(\theta_i)$ is the relative time delay at array element l for source i with θ_i being the direction of arrival for source i, $n_l(k)$ is a complex-valued Gaussian white noise with $E[|n_l(k)|^2] = 2\sigma_n^2$, A_i is the narrow-band channel coefficient for user i, $\bar{x}_l(k)$ denotes the noiseless part of $x_l(k)$ and $b_i(k)$ is the k-th symbol of user i which takes the value from the M-QAM symbol set

$$\mathcal{B} \triangleq \{b_{l,q} = u_l + ju_q, \ 1 \leq l, q \leq \sqrt{M}\} \tag{2}$$

with the real-part symbol $\Re[b_{l,q}] = u_l = 2l - \sqrt{M} - 1$ and the imaginary-part symbol $\Im[b_{l,q}] = u_q = 2q - \sqrt{M} - 1$. Assume that source 1 is the desired user and the rest of the sources are interfering users. The desired-user signal-to-noise ratio (SNR) is given by SNR$= |A_1|^2 \sigma_b^2 / 2\sigma_n^2$ and the desired signal-to-interferer i ratio (SIR) is SIR$_i = A_1^2/A_i^2$, for $2 \leq i \leq S$, where σ_b^2 denotes the M-QAM symbol energy. The received signal vector $\mathbf{x}(k) = [x_1(k) \ x_2(k) \cdots x_L(k)]^T$ can be expressed as

$$\mathbf{x}(k) = \mathbf{P}\mathbf{b}(k) + \mathbf{n}(k) = \bar{\mathbf{x}}(k) + \mathbf{n}(k), \tag{3}$$

where $\mathbf{n}(k) = [n_1(k) \ n_2(k) \cdots n_L(k)]^T$, the system matrix $\mathbf{P} = [A_1\mathbf{s}_1 \ A_2\mathbf{s}_2 \cdots A_S\mathbf{s}_S]$ with the steering vector for source i given by $\mathbf{s}_i = [e^{j\omega t_1(\theta_i)} \ e^{j\omega t_2(\theta_i)} \cdots e^{j\omega t_L(\theta_i)}]^T$, and the transmitted QAM symbol vector $\mathbf{b}(k) = [b_1(k) \ b_2(k) \cdots b_S(k)]^T$.

Before it is proceeded further, the assumptions implied for the above system model are explained and justified. Although a linear antenna array structure with uniformly spaced elements is assumed, the approach is actually more general, and it is equally applicable to the generic narrow-band multiple-input multiple-output (MIMO) system [12],[14] modelled by $\mathbf{x}(k) = \mathbf{P}\mathbf{b}(k) + \mathbf{n}(k)$, where the (l, i)-th element of the channel matrix $\mathbf{P}$ represents the non-dispersive channel connecting the i-th transmit antenna to the l-th receive antenna. Except for the reference

user's channel coefficient A_1 and steering vector $\mathbf{s}_1$, the receiver does not need to know the interfering users' channel coefficients A_i and steering vector $\mathbf{s}_i$, $2 \leq i \leq S$. The adaptive beamforming approach considered is based on the so-called temporal reference technique, and during the training the reference user's transmitted symbols are available at the receiver for the adaptation purpose. The receiver, however, does not have access to the interfering users' data symbols. As will be explained latter, the first column $\mathbf{p}_1$ of the system matrix $\mathbf{P}$, corresponding to the desired user, is required at the receiver in order to detect the desired user's data symbols unbiasedly.

In the system model (3), the desired user and interfering signals are assumed to be symbol-synchronised. For the downlink scenario synchronous transmission of the users is guaranteed. By contrast, in an uplink scenario the differently delayed asynchronous signals of the users are no longer automatically synchronised. However, the quasi-synchronous operation of the system may be achieved with the aid of adaptive timing advance control, as in the global system of mobile (GSM) communications [31]. The GSM system has a timing-advance control accuracy of 0.25 bit duration. Since synchronous systems perform better than their asynchronous counterparts [32], the third-generation partnership research consortium (3GPP) is also considering the employment of timing-advance control in next-generation systems. In general, when the number of users is large, the users are asynchronous and the idealistic assumption of perfect power control is stipulated, the performance gain of the (symbol-rate) MSER solution over the MMSE beamformer may be expected to diminish, since the interference becomes nearly Gaussian at the symbol-rate samples. One way of maintaining the benefits of the MSER solution for asynchronous systems is to perform a joint MSER detection and synchronisation by sampling faster than the symbol rate. During each symbol period, several signal samples are taken and the receiver maintains several tentative MSER detectors. The detector having the smallest SER is chosen to perform symbol detection. In this study, symbol-rate synchronisation is assumed. For such a symbol-synchronised interference-limited QAM system the non-Gaussian nature of the interfering signals is effectively exploited by the MSER beamforming receiver, resulting in an improved SER performance.

A beamformer is employed at the receiver, whose soft output is given by

$$y(k) = \mathbf{w}^H \mathbf{x}(k) = \mathbf{w}^H (\bar{\mathbf{x}}(k) + \mathbf{n}(k)) = \bar{y}(k) + e(k), \tag{4}$$

where $\mathbf{w} = [w_1 \ w_2 \cdots w_L]^T$ is the complex-valued beamformer weight vector and $e(k)$ is

Gaussian distributed with zero mean and $E[|e(k)|^2] = 2\sigma_n^2 \mathbf{w}^H \mathbf{w}$. Define the combined system impulse response of the channel and beamformer as $\mathbf{w}^H \mathbf{P} = \mathbf{w}^H [\mathbf{p}_1 \ \mathbf{p}_2 \cdots \mathbf{p}_S] = [c_1 \ c_2 \cdots c_S]$. The beamformer's output can alternatively be expressed as

$$y(k) = c_1 b_1(k) + \sum_{i=2}^{S} c_i b_i(k) + e(k), \tag{5}$$

where the first term in the righthand side of equation is the desired user signal and the second term is the residual multiuser interference. Note that, in any detection scheme, the main tap c_1 must be known. That is, the desired user's channel and associated steering vector, namely $\mathbf{p}_1 = A_1 \mathbf{s}_1$, must be known at the receiver. If this fact is overlooked, the decision will be biased [33]. Provided that $c_1 = c_{R_1} + jc_{I_1}$ satisfies $c_{R_1} > 0$ and $c_{I_1} = 0$, the symbol decision $\hat{b}_1(k) = \hat{b}_{R_1}(k) + j\hat{b}_{I_1}(k)$ can be made as

$$\hat{b}_{R_1}(k) = \begin{cases} u_1, & \text{if } y_R(k) \leq c_{R_1}(u_1 + 1), \\ u_l, & \text{if } c_{R_1}(u_l - 1) < y_R(k) \leq c_{R_1}(u_l + 1) \\ & \text{for } 2 \leq l \leq \sqrt{M} - 1, \\ u_{\sqrt{M}}, & \text{if } y_R(k) > c_{R_1}(u_{\sqrt{M}} - 1), \end{cases} \tag{6}$$

$$\hat{b}_{I_1}(k) = \begin{cases} u_1, & \text{if } y_I(k) \leq c_{R_1}(u_1 + 1), \\ u_q, & \text{if } c_{R_1}(u_q - 1) < y_I(k) \leq c_{R_1}(u_q + 1) \\ & \text{for } 2 \leq q \leq \sqrt{M} - 1, \\ u_{\sqrt{M}}, & \text{if } y_I(k) > c_{R_1}(u_{\sqrt{M}} - 1), \end{cases} \tag{7}$$

where $y(k) = y_R(k) + jy_I(k)$ and $\hat{b}_1(k)$ is the estimate for $b_1(k) = b_{R_1}(k) + jb_{I_1}(k)$. Fig. 1 depicts the decision thresholds associated with the decision $\hat{b}_1(k) = b_{l,q}$. In general, $c_1 = \mathbf{w}^H \mathbf{p}_1$ is complex-valued and the rotating operation

$$\mathbf{w}^{\text{new}} = \frac{c_1^{\text{old}}}{\left| c_1^{\text{old}} \right|} \mathbf{w}^{\text{old}} \tag{8}$$

can be used to make c_1 real and positive. This rotation is a linear operation and it does not change the system's SER.

III. ADAPTIVE BEAMFORMING ASSISTED RECEIVERS

Different beamforming designs derive the beamformer's weight vector $\mathbf{w}$ based on optimising different design criteria. The best-known design criterion is the MMSE criterion, while the novelty of this constribution is to optimise the beamformer's weight vector based on the MSER criterion. The MMSE and MSER designs are considered in this contribution.
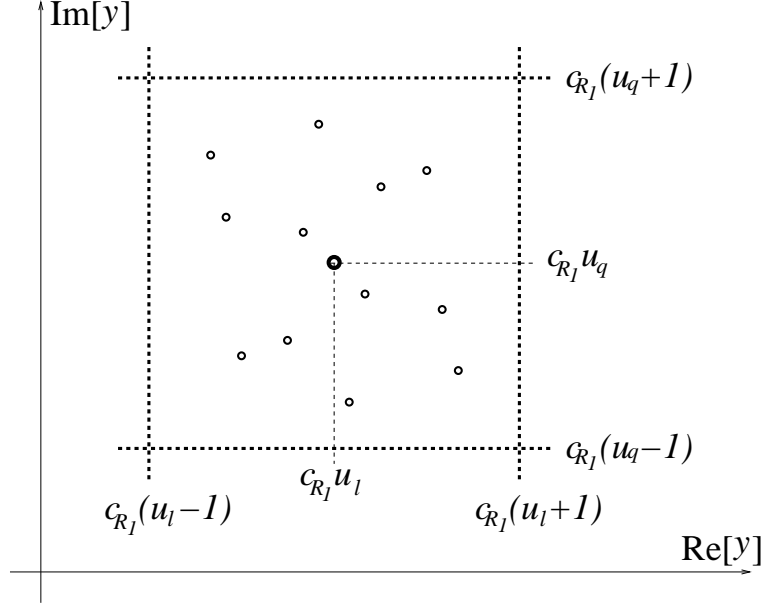
Fig. 1. Decision thresholds associated with point $c_1 b_{l,q}$ assuming $c_{R_1} > 0$ and $c_{I_1} = 0$, and illustrations of symmetric distribution of $y_{l,q}$ around $c_1 b_{l,q}$.

A. Minimum Mean Square Error Beamforming Design

The traditional design for the beamformer (4) is the MMSE solution, which minimises the MSE criterion $E[|b_1(k) - y(k)|^2]$, leading to the solution for the weight vector given by

$$\mathbf{w}_{\text{MMSE}} = \left(\mathbf{P}\mathbf{P}^H + \frac{2\sigma_n^2}{\sigma_b^2}\mathbf{I}_L \right)^{-1} \mathbf{p}_1, \tag{9}$$

where $\mathbf{I}_L$ denotes the $L \times L$ identity matrix. The MMSE beamforming design is computationally attractive, because it admits the closed-form solution given the second order statistics of the underlying system. Furthermore, it can be implemented adaptively using the classical LMS algorithm [20],[21]. Given the current beamformer's output $y(k) = \hat{\mathbf{w}}^H(k)\mathbf{x}(k)$, the LMS algorithm modified for the adaptation of the QAM beamformer (4) is expressed as

$$\tilde{\mathbf{w}}(k+1) = \hat{\mathbf{w}}(k) + \mu \left(b_1(k) - y(k) \right)^* \mathbf{x}(k), \tag{10}$$

$$\tilde{c}_1(k+1) = \tilde{\mathbf{w}}^H(k+1)\hat{\mathbf{p}}_1, \tag{11}$$

$$\hat{\mathbf{w}}(k+1) = \frac{\tilde{c}_1(k+1)}{|\tilde{c}_1(k+1)|}\tilde{\mathbf{w}}(k+1), \tag{12}$$

where μ is a small positive step size, $\hat{\mathbf{p}}_1$ is an estimate of $\mathbf{p}_1$, and (11) and (12) implement the weight rotation operation. Given a training data block $\{b_1(k), \mathbf{x}(k)\}_{k=1}^N$, a block-based estimate

of $\mathbf{p}_1$ is given by

$$\hat{\mathbf{p}}_1 = \frac{1}{N} \sum_{k=1}^{N} \frac{\mathbf{x}(k)}{b_1(k)}. \tag{13}$$

Alternatively, the receiver can track $\mathbf{p}_1$ using the simple moving average

$$\hat{\mathbf{p}}_1(k+1) = (1-\alpha)\hat{\mathbf{p}}_1(k) + \alpha \frac{\mathbf{x}(k)}{b_1(k)}, \tag{14}$$

where $0 < \alpha < 1$ is a positive step size. Note that $\hat{c}_1(k) = \hat{\mathbf{w}}^H(k)\hat{\mathbf{p}}_1$ is real-valued and positive.

B. Minimum Symbol Error Rate Beamforming Design

Since the SER is the true performance indicator, it is desired to consider the optimal MSER Beamforming solution. Denote the $N_b = M^S$ number of legitimate sequences of $\mathbf{b}(k)$ as $\mathbf{b}_i$, $1 \leq i \leq N_b$. The noise-free part of the received signal $\bar{\mathbf{x}}(k)$ takes values from the signal set defined by $\mathcal{X} \triangleq \{\bar{\mathbf{x}}_i = \mathbf{P}\mathbf{b}_i, \ 1 \leq i \leq N_b\}$. The set $\mathcal{X}$ can be partitioned into M subsets, depending on the value of $b_1(k)$ as $\mathcal{X}_{l,q} \triangleq \{\bar{\mathbf{x}}_i \in \mathcal{X} : \ b_1(k) = b_{l,q}\}, \ 1 \leq l, q \leq \sqrt{M}$. Similarly the noise-free part of the beamformer's output $\bar{y}(k)$ takes values from the scalar set $\mathcal{Y} \triangleq \{\bar{y}_i = \mathbf{w}^H \bar{\mathbf{x}}_i, \ 1 \leq i \leq N_b\}$, and $\mathcal{Y}$ can be divided into the M subsets conditioned on $b_1(k)$

$$\mathcal{Y}_{l,q} \triangleq \{\bar{y}_i \in \mathcal{Y} : \ b_1(k) = b_{l,q}\}, \ 1 \leq l, q \leq \sqrt{M}. \tag{15}$$

The following two lemmas summarise the properties of the signal subsets $\mathcal{Y}_{l,q}$, $1 \leq l, q \leq \sqrt{M}$, which are useful in the derivation of the SER expression for the beamformer (4).

Lemma 1: The subsets $\mathcal{Y}_{l,q}$, $1 \leq l, q \leq \sqrt{M}$, satisfy the shifting properties

$$\mathcal{Y}_{l+1,q} = \mathcal{Y}_{l,q} + 2c_1, \ 1 \leq l \leq \sqrt{M} - 1, \tag{16}$$

$$\mathcal{Y}_{l,q+1} = \mathcal{Y}_{l,q} + j2c_1, \ 1 \leq q \leq \sqrt{M} - 1, \tag{17}$$

$$\mathcal{Y}_{l+1,q+1} = \mathcal{Y}_{l,q} + (2+j2)c_1, \ 1 \leq l, q \leq \sqrt{M} - 1. \tag{18}$$

Proof: Any point $\bar{y}_i^{(l+1,q)} \in \mathcal{Y}_{l+1,q}$ can be expressed as

$$\bar{y}_i^{(l+1,q)} = \mathbf{w}^H \mathbf{P} \mathbf{b}_i^{(l+1,q)} = \mathbf{w}^H \mathbf{P} \left(\mathbf{b}_i^{(l,q)} + [2 \ 0 \cdots 0]^T \right) = \bar{y}_i^{(l,q)} + 2c_1$$

where $\bar{y}_i^{(l,q)} \in \mathcal{Y}_{l,q}$. This proves the shifting property (16). Proofs for the other two equations are similar.

Lemma 2: The points of $\mathcal{Y}_{l,q}$ are distributed symmetrically around the symbol point $c_1 b_{l,q}$. This symmetric distribution is with respect to the two horizontal decision boundaries and the two vertical decision boundaries that separate $\mathcal{Y}_{l,q}$ from the other subsets.

Lemma 2 is a direct consequence of symmetric distribution of the symbol constellation (2) and Lemma 1. This symmetric property is also illustrated in Fig. 1.

For the beamformer with weight vector $\mathbf{w}$, denote

$$P_E(\mathbf{w}) = \text{Prob}\{\hat{b}_1(k) \neq b_1(k)\}, \tag{19}$$

$$P_{E_R}(\mathbf{w}) = \text{Prob}\{\hat{b}_{R_1}(k) \neq b_{R_1}(k)\}, \tag{20}$$

$$P_{E_I}(\mathbf{w}) = \text{Prob}\{\hat{b}_{I_1}(k) \neq b_{I_1}(k)\}. \tag{21}$$

$P_E(\mathbf{w})$ is the total SER, while $P_{E_R}(\mathbf{w})$ and $P_{E_I}(\mathbf{w})$ are the real-part and imaginary-part SERs, respectively. It is then easy to see that the SER is given by

$$P_E(\mathbf{w}) = P_{E_R}(\mathbf{w}) + P_{E_I}(\mathbf{w}) - P_{E_R}(\mathbf{w})P_{E_I}(\mathbf{w}). \tag{22}$$

From the beamforming model (4) and the signal model (3), the conditional probability density function (PDF) of $y(k)$ given $b_1(k) = b_{l,q}$ is a Gaussian mixture (hence a non-Gaussian PDF) defined by

$$p(y|b_{l,q}) = \frac{1}{N_{sb}2\pi\sigma_n^2\mathbf{w}^H\mathbf{w}} \sum_{i=1}^{N_{sb}} e^{-\frac{|y-\bar{y}_i^{(l,q)}|^2}{2\sigma_n^2\mathbf{w}^H\mathbf{w}}}, \tag{23}$$

where $N_{sb} = N_b/M$ is the size of $\mathcal{Y}_{l,q}$, $\bar{y}_i^{(l,q)} = \bar{y}_{R_i}^{(l,q)} + j\bar{y}_{I_i}^{(l,q)} \in \mathcal{Y}_{l,q}$, and $y = y_R + jy_I$. Noting that c_1 is real-valued and positive and taking into account the symmetric distribution of $\mathcal{Y}_{l,q}$ (Lemma 2), for $2 \leq l \leq \sqrt{M} - 1$, the conditional error probability of $\hat{b}_{R_1}(k) \neq u_l$ given $b_{R_1}(k) = u_l$ can be shown to be [34]

$$P_{E_R,l}(\mathbf{w}) = \frac{2}{N_{sb}} \sum_{i=1}^{N_{sb}} Q(g_{R_i}^{(l,q)}(\mathbf{w})), \tag{24}$$

where

$$Q(u) = \frac{1}{\sqrt{2\pi}} \int_u^\infty e^{-\frac{z^2}{2}} dz, \tag{25}$$

and

$$g_{R_i}^{(l,q)}(\mathbf{w}) = \frac{\bar{y}_{R_i}^{(l,q)} - c_{R_1}(u_l - 1)}{\sigma_n\sqrt{\mathbf{w}^H\mathbf{w}}}. \tag{26}$$

Further taking into account the shifting property (Lemma 1), it can be shown that

$$P_{E_R}(\mathbf{w}) = \gamma \frac{1}{N_{sb}} \sum_{i=1}^{N_{sb}} Q(g_{R_i}^{(l,q)}(\mathbf{w})), \tag{27}$$

where $\gamma = \frac{2\sqrt{M}-2}{\sqrt{M}}$. It is seen that P_{E_R} can be evaluated using (real part of) any single subset $\mathcal{Y}_{l,q}$. Similarly, P_{E_I} can be evaluated using (imaginary part of) any single subset $\mathcal{Y}_{l,q}$ as

$$P_{E_I}(\mathbf{w}) = \gamma \frac{1}{N_{sb}} \sum_{i=1}^{N_{sb}} Q(g_{I_i}^{(l,q)}(\mathbf{w})) \tag{28}$$

with

$$g_{I_i}^{(l,q)}(\mathbf{w}) = \frac{\bar{y}_{I_i}^{(l,q)} - c_{R_1}(u_q - 1)}{\sigma_n \sqrt{\mathbf{w}^H \mathbf{w}}}. \tag{29}$$

Note that the SER is invariant to a positive scaling of $\mathbf{w}$.

The MSER solution $\mathbf{w}_{\mathrm{MSER}}$ is defined as the weight vector that minimises the upper bound of the SER given by

$$P_{E_B}(\mathbf{w}) = P_{E_R}(\mathbf{w}) + P_{E_I}(\mathbf{w}), \tag{30}$$

that is,

$$\mathbf{w}_{\mathrm{MSER}} = \arg \min_{\mathbf{w}} P_{E_B}(\mathbf{w}). \tag{31}$$

The solution obtained by minimising the upper bound (30) is practically equivalent to that of minimising $P_E(\mathbf{w})$, since the bound $P_E(\mathbf{w}) < P_{E_B}(\mathbf{w})$ is very tight, that is, $P_{E_B}(\mathbf{w})$ is very close to the true SER $P_E(\mathbf{w})$. Unlike the MMSE solution, the MSER solution does not admits a closed-form solution. However, the gradients of $P_{E_R}(\mathbf{w})$ and $P_{E_I}(\mathbf{w})$ with respect to $\mathbf{w}$ can be shown to be respectively

$$\nabla P_{E_R}(\mathbf{w}) = \frac{\gamma}{2 N_{sb} \sqrt{2\pi} \sigma_n \sqrt{\mathbf{w}^H \mathbf{w}}} \sum_{i=1}^{N_{sb}} e^{-\frac{\left(\bar{y}_{R_i}^{(l,q)} - c_{R_1}(u_l - 1)\right)^2}{2\sigma_n^2 \mathbf{w}^H \mathbf{w}}}$$
$$\times \left(\frac{\bar{y}_{R_i}^{(l,q)} - c_{R_1}(u_l - 1)}{\mathbf{w}^H \mathbf{w}} \mathbf{w} - \bar{\mathbf{x}}_i^{(l,q)} + (u_l - 1)\mathbf{p}_1 \right), \tag{32}$$

$$\nabla P_{E_I}(\mathbf{w}) = \frac{\gamma}{2 N_{sb} \sqrt{2\pi} \sigma_n \sqrt{\mathbf{w}^H \mathbf{w}}} \sum_{i=1}^{N_{sb}} e^{-\frac{\left(\bar{y}_{I_i}^{(l,q)} - c_{R_1}(u_q - 1)\right)^2}{2\sigma_n^2 \mathbf{w}^H \mathbf{w}}}$$
$$\times \left(\frac{\bar{y}_{I_i}^{(l,q)} - c_{R_1}(u_q - 1)}{\mathbf{w}^H \mathbf{w}} \mathbf{w} + j\bar{\mathbf{x}}_i^{(l,q)} + (u_q - 1)\mathbf{p}_1 \right), \tag{33}$$

where $\bar{\mathbf{x}}_i^{(l,q)} \in \mathcal{X}_{l,q}$. With the gradient $\nabla P_{E_B}(\mathbf{w}) = \nabla P_{E_R}(\mathbf{w}) + \nabla P_{E_I}(\mathbf{w})$, the optimisation problem (31) can be solved iteratively using a gradient-based algorithm. Since the SER is

invariant to a positive scaling of $\mathbf{w}$, it is computationally advantageous to normalise $\mathbf{w}$ to a unit-length vector $\check{\mathbf{w}}$ after every iteration, so that the gradients (32) and (33) are simplified to

$$\nabla P_{E_R}(\check{\mathbf{w}}) = \frac{\gamma}{2N_{sb}\sqrt{2\pi}\sigma_n} \sum_{i=1}^{N_{sb}} e^{-\frac{\left(\bar{y}_{R_i}^{(l,q)} - c_{R_1}(u_l-1)\right)^2}{2\sigma_n^2}}$$
$$\times \left(\left(\bar{y}_{R_i}^{(l,q)} - c_{R_1}(u_l-1)\right)\check{\mathbf{w}} - \bar{\mathbf{x}}_i^{(l,q)} + (u_l-1)\mathbf{p}_1\right) \tag{34}$$

and

$$\nabla P_{E_I}(\check{\mathbf{w}}) = \frac{\gamma}{2N_{sb}\sqrt{2\pi}\sigma_n} \sum_{i=1}^{N_{sb}} e^{-\frac{\left(\bar{y}_{I_i}^{(l,q)} - c_{R_1}(u_q-1)\right)^2}{2\sigma_n^2}}$$
$$\times \left(\left(\bar{y}_{I_i}^{(l,q)} - c_{R_1}(u_q-1)\right)\check{\mathbf{w}} + j\bar{\mathbf{x}}_i^{(l,q)} + (u_q-1)\mathbf{p}_1\right). \tag{35}$$

The following algorithm, which is a modified version of the simplified conjugate gradient algorithm of [35],[36], provides an efficient means of finding an MSER solution.

- *Initialisation.* Choose a step size of $\mu > 0$ and a termination scalar of $\beta > 0$; given $\check{\mathbf{w}}(1)$ and $\mathbf{d}(1) = -\nabla P_{E_B}(\check{\mathbf{w}}(1))$; set the iteration index to $\iota = 1$.
- *Loop.* If $\|\nabla P_{E_B}(\check{\mathbf{w}}(\iota))\| = \sqrt{(\nabla P_{E_B}(\check{\mathbf{w}}(\iota)))^H \nabla P_{E_B}(\check{\mathbf{w}}(\iota))} < \beta$: goto *Stop*. Else,

$$\tilde{\mathbf{w}}(\iota+1) = \check{\mathbf{w}}(\iota) + \mu \mathbf{d}(\iota),$$

$$c_1(\iota+1) = \tilde{\mathbf{w}}^H(\iota+1)\mathbf{p}_1,$$

$$\bar{\mathbf{w}}(\iota+1) = \frac{c_1(\iota+1)}{|c_1(\iota+1)|}\tilde{\mathbf{w}}(\iota+1),$$

$$\check{\mathbf{w}}(\iota+1) = \frac{\bar{\mathbf{w}}(\iota+1)}{\|\bar{\mathbf{w}}(\iota+1)\|},$$

$$\phi_\iota = \frac{\|\nabla P_{E_B}(\check{\mathbf{w}}(\iota+1))\|^2}{\|\nabla P_{E_B}(\check{\mathbf{w}}(\iota))\|^2},$$

$$\mathbf{d}(\iota+1) = \phi_\iota \mathbf{d}(\iota) - \nabla P_{E_B}(\check{\mathbf{w}}(\iota+1)),$$

$\iota = \iota + 1$, goto *Loop*.

- *Stop.* $\check{\mathbf{w}}(\iota)$ is the solution.

At a minimum, $\|\nabla P_{E_B}(\check{\mathbf{w}})\| = 0$. Hence the termination scalar β determines the accuracy of the solution obtained. The step size μ controls the rate of convergence. Typically, a much larger value of μ can be used compared to the steepest-descent gradient algorithm. As the SER surface $P_{E_B}(\check{\mathbf{w}})$ is highly nonlinear, occasionally the search direction $\mathbf{d}$ may no longer be a good

approximation to the conjugate gradient direction or may even point to the "uphill" direction, when the iteration index becomes large. It is thus advisable to periodically reset $\mathbf{d}$ to the negative gradient in the above conjugate gradient algorithm. With this resetting mechanism, this conjugate gradient algorithm has been shown to converge fast to the theoretical MSER solution, typically in tens of iterations, in many simulation studies. Although in theory there is no guarantee that the above conjugate gradient algorithm can always find the global minimum point of the SER surface $P_{E_B}(\breve{\mathbf{w}})$, in practice we have found that the algorithm works well and we have never observed any occurrence of the algorithm being trapped at some local minimum solution.

It is worth emphasising that there exist infinitely many global MSER solutions which forms an infinite half line in the beamforming weight space. This is because the SER is invariant to a positive scaling of $\mathbf{w}$, i.e. the size of $\mathbf{w}$ does not matter (except for zero size). Thus, the SER surface has an infinitely long valley, and any point at the bottom of this valley is a true global MSER solution. For an illustration, see the simple example given in [36]. Once we restrict to the unit-length $\breve{\mathbf{w}}$, the MSER solution becomes unique. As alternatives to the simplified conjugate gradient algorithm, global optimisation search algorithms, such as the genetic algorithm [37],[38] and adaptive simulated annealing [39],[40], can be used to obtain a global minimum solution of $P_{E_B}(\mathbf{w})$, at an expense of considerably increased computational requirements.

C. Adaptive Minimum Symbol Error Rate Beamforming

In practice, the system matrix $\mathbf{P}$ is unknown (except its first column). Therefore adaptive implementation is required to realise the MSER beamforming. To adaptively implement the MMSE solution, the unknown second-order statistics can be estimated based on a block of training data. Furthermore, by considering a single-sample "estimate" of the MSE, the stochastic adaptive algorithm known as the LMS algorithm is derived. A similar adaptive implementation strategy can be adopted for adaptive MSER beamforming. The PDF $p(y)$ of $y(k)$ can be estimated using the Parzen window estimate [41]-[43] based on a block of training data. This leads to an estimated SER for the beamformer. Minimising this estimated SER based on a gradient optimisation yields an approximated MSER solution. To derive a sample-by-sample adaptive algorithm, consider a single-sample "estimate" of $p(y)$

$$\tilde{p}(y,k) = \frac{1}{2\pi\rho_n^2} e^{-\frac{|y-y(k)|^2}{2\rho_n^2}} \tag{36}$$

and the corresponding one-sample SER "estimate" $\tilde{P}_{E_B}(\mathbf{w}, k)$. The parameter ρ_n is known as the kernel width. Using the instantaneous stochastic gradient of $\nabla \tilde{P}_{E_B}(\mathbf{w}, k) = \nabla \tilde{P}_{E_R}(\mathbf{w}, k) + \nabla \tilde{P}_{E_I}(\mathbf{w}, k)$ with

$$
\begin{aligned}
\nabla \tilde{P}_{E_R}(\mathbf{w}, k) = \frac{\gamma}{2\sqrt{2\pi}\rho_n} e^{-\frac{\left(y_R(k) - \hat{c}_{R_1}(k)(b_{R_1}(k) - 1)\right)^2}{2\rho_n^2}} \\
\times \left(-\mathbf{x}(k) + (b_{R_1}(k) - 1)\hat{\mathbf{p}}_1\right)
\end{aligned}
\tag{37}
$$

and

$$
\begin{aligned}
\nabla \tilde{P}_{E_I}(\mathbf{w}, k) = \frac{\gamma}{2\sqrt{2\pi}\rho_n} e^{-\frac{\left(y_I(k) - \hat{c}_{R_1}(k)(b_{I_1}(k) - 1)\right)^2}{2\rho_n^2}} \\
\times \left(j\mathbf{x}(k) + (b_{I_1}(k) - 1)\hat{\mathbf{p}}_1\right)
\end{aligned}
\tag{38}
$$

gives rise to the stochastic gradient adaptive algorithm referred to as the least symbol error rate (LSER) algorithm

$$
\tilde{\mathbf{w}}(k + 1) = \hat{\mathbf{w}}(k) + \mu \left(-\nabla \tilde{P}_{E_B}(\hat{\mathbf{w}}(k), k)\right),
\tag{39}
$$

$$
\tilde{c}_1(k + 1) = \tilde{\mathbf{w}}^H(k + 1)\hat{\mathbf{p}}_1,
\tag{40}
$$

$$
\hat{\mathbf{w}}(k + 1) = \frac{\tilde{c}_1(k + 1)}{|\tilde{c}_1(k + 1)|}\tilde{\mathbf{w}}(k + 1).
\tag{41}
$$

The rotating operation (40) and (41) ensures that $\hat{c}_1(k) \triangleq \hat{\mathbf{w}}^H(k)\hat{\mathbf{p}}_1 = \hat{c}_{R_1}(k) + j\hat{c}_{I_1}(k)$ satisfies $\hat{c}_{R_1}(k) > 0$ and $\hat{c}_{I_1}(k) = 0$. The step size μ and the kernel width ρ_n are the two algorithmic parameters that should be set appropriately in order to ensure an adequate performance in terms of convergence rate and steady-state SER misadjustment. Note that there is no need to normalise the weight vector after each updating. That is, it does not restrict to the unit-length solution. The estimate of $\mathbf{p}_1$ can be provided by either (13) or (14).

Theoretical proof for convergence of this LSER algorithm is very difficult if not impossible and it is still under investigation. However, it can be pointed out that this LSER algorithm belongs to the general stochastic gradient-based adaptive algorithm investigated in [44]. Therefore, the results of local convergence analysis presented in [44] is applicable here. Our previous investigations [1],[34] have suggested that the LSER algorithm behaves well, has a reasonable convergence speed, and is consistently outperforms the LMS algorithm in terms of the achievable SER. Influence of the two algorithmic parameters of the LSER algorithm, namely μ and ρ_n, to the SER performance will be investigated in the following simulation.
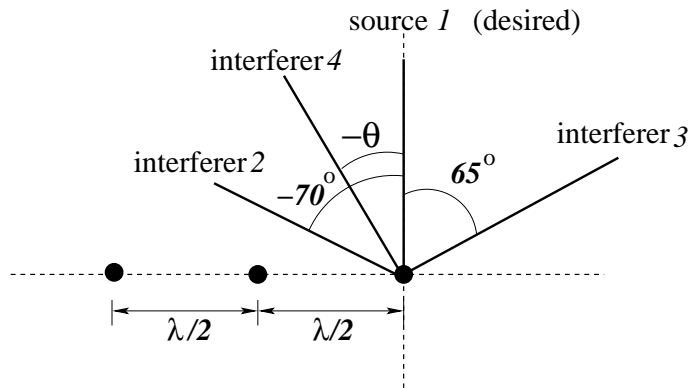
Fig. 2. Locations of the user sources with respect to the three-element linear array with $\lambda/2$ element spacing, λ being the wavelength, where $\theta < 65°$.

IV. SIMULATION STUDY

The prototype system investigated consisted of four sources and a three-element antenna array. Fig. 2 shows the locations of the desired source and the interfering sources graphically, where the angular separation between the desired user and the interfering user 4 was $\theta < 65°$. Note that the performance of a beamforming receiver mainly depends on the minimum angular separation between the desired user and the interfering users (in this case θ), and whether or not the desired user is at the broadside of the antenna array is not critical at all. As emphasised in Section II, the column of the system matrix associated with the desired user, namely $\mathbf{p}_1$, must be known in receiver. Usually, $\mathbf{p}_1$ can be estimated accurately during training. Thus, in the following simulation study, a perfect $\mathbf{p_1}$ is assumed at receiver.

A. Stationary System

The modulation scheme was 16-QAM and all the channels A_i, $1 \le i \le 4$, were time-invariant. Fig. 3 compares the SER performance of the MSER beamforming solution to that of the MMSE beamforming solution under four different conditions: (**a**) the minimum anugular separation between the desired user 1 and the interfering user 4 was $\theta = 32°$, and all the four users had an equal signal power, i.e. $\text{SIR}_i = 0$ dB for $2 \le i \le 4$; (**b**) $\theta = 30°$, and all the four users had an equal signal power; (**c**) $\theta = 28°$, and all the four users had an equal signal power; and (**d**) $\theta = 30°$, user 1 and user 2 had the same signal power but users 3 and 4 had 2 dB more power than users 1 and 2, i.e. $\text{SIR}_2 = 0$ dB and $\text{SIR}_3 = \text{SIR}_4 = -2$ dB. The MMSE beamformer was
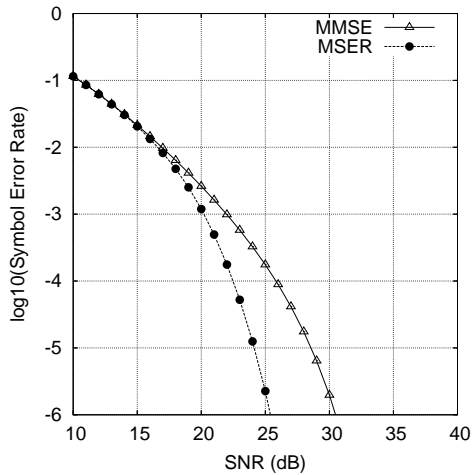
(a) $\theta = 32°$, $\text{SIR}_i = 0$ dB, $2 \le i \le 4$
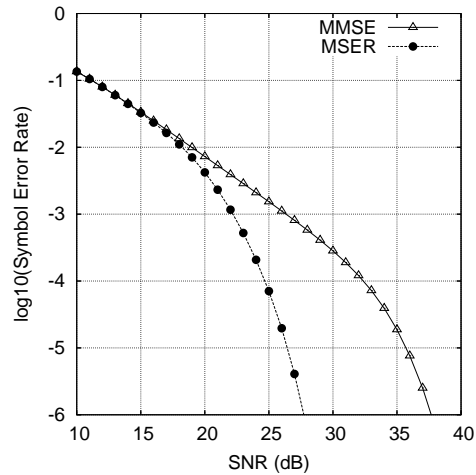
(b) $\theta = 30°$, $\text{SIR}_i = 0$ dB, $2 \le i \le 4$
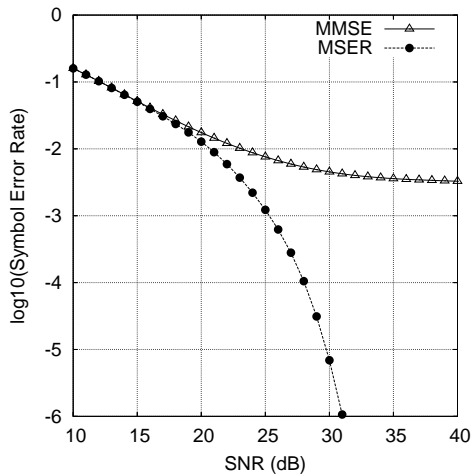
(c) $\theta = 28°$, $\text{SIR}_i = 0$ dB, $2 \le i \le 4$
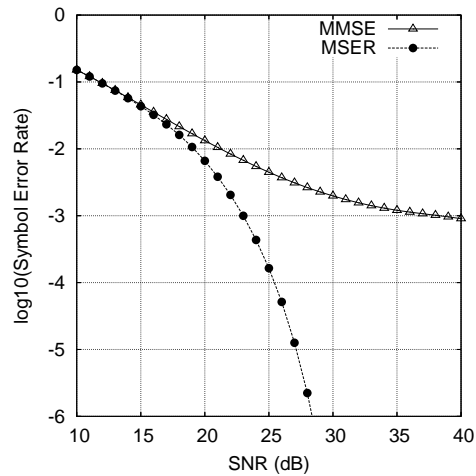
(d) $\theta = 30°$, $\text{SIR}_2 = 0$ dB, $\text{SIR}_3 = \text{SIR}_4 = -2$ dB

Fig. 3. Desired user's symbol error rate performance comparison for the non-fading channel system employing the three-element array of Fig. 2 to support four 16-QAM users.

provided by the closed-form solution (9), while the MSER solution was obtained numerically using the conjugate gradient algorithm.

For the case of equal user power with the minimum anugular separation $\theta = 32°$, the MSER beamforming solution had an SNR gain of 2 dB over the MMSE solution at the SER level of 10^{-3}, as can be seen from Fig. 3 (a). When the minimum anugular separation of the system was reduced to $\theta = 30°$, as depicted in Fig. 3 (b), the SNR gain of the MSER beamformer over the MMSE one was increased to 4 dB. With the minimum anugular separation further reduced to $\theta = 28°$, the MMSE beamforming solution became incapable of removing the interference and exhibited

a high SER floor, as illustrated in Fig. 3 (c). In contrast, the MSER beamformer remained capable of effectively removing the interference and achieving an adequate SER performance. By comparing Fig. 3 (b) with Fig. 3 (d), it can be seen that, with the minimum anugular separation $\theta = 30°$ and when facing stronger interfering users 3 and 4, the MMSE solution faltered while the MSER solution suffered from very little degradation. This clearly demonstrated that the MSER beamformer is more robust in near-far situations than the MMSE beamformer.

The MSER solution is defined as the weight vector that minimises the upper bound SER $P_{E_B}(\mathbf{w}) = P_{E_R}(\mathbf{w}) + P_{E_I}(\mathbf{w})$, and in Section III-B it is pointed out that this is practically equivalent to minimise the true SER. The true SER is given by the sum of the inphase and quadrature components' error rates minus the appropriate correction term used for preventing the "double-counting" error-events as follows $P_E(\mathbf{w}) = P_{E_R}(\mathbf{w}) + P_{E_I}(\mathbf{w}) - P_{E_R}(\mathbf{w})P_{E_I}(\mathbf{w})$. The probability of simultaneous inphase and quadrature errors, which is represented by the term $P_{E_R}(\mathbf{w})P_{E_I}(\mathbf{w})$ tends to be quite low, unless the SNR is extremely low. More explicitly, the last term is typically orders of magnitude lower than the first two terms. Hence the bound $P_E(\mathbf{w}) < P_{E_B}(\mathbf{w})$ is very tight, i.e. $P_{E_B}(\mathbf{w})$ is very close to $P_E(\mathbf{w})$. In fact, $P_{E_B}(\mathbf{w})$ is almost indistinguishable from $P_E(\mathbf{w})$. This is not surprising, since the term $P_{E_R}(\mathbf{w})P_{E_I}(\mathbf{w})$ is negligible in comparison to the dominant term $P_{E_R}(\mathbf{w}) + P_{E_I}(\mathbf{w})$. For example, when $P_{E_R}(\mathbf{w})$ or $P_{E_I}(\mathbf{w})$
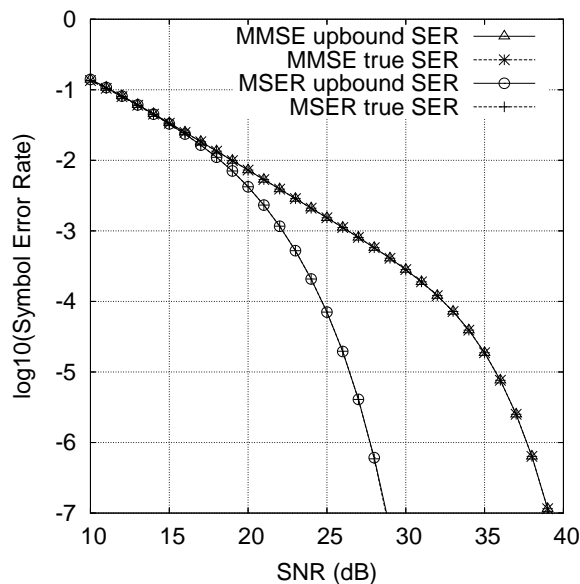

Fig. 4.   Comparison of the true symbol error rate and its upper bound for the non-fading channel system employing the three-element array of Fig. 2 with a minimum angular separation of $\theta = 30°$ to support four equal-power 16-QAM users.

(they are symmetric) is of the order of 10^{-2}, then $P_{E_R}(\mathbf{w})P_{E_I}(\mathbf{w})$ is of the order of 10^{-4}, which constitutes an almost negligible factor. This is confirmed by the results of Fig. 4, where both the true SER $P_E(\mathbf{w})$ and its upper bound $P_{E_B}(\mathbf{w})$ are plotted for the MMSE and MSER solutions under the channel conditions of $\theta = 30°$ and equal user power.

Both the LMS and LSER based adaptive beamforming algorithms were next investigated using the system of the minimum angular separation $\theta = 30°$, equal user power and SNR= 26 dB. Given $\hat{\mathbf{w}}(0) = [0.1 + j0.1 \quad 0.1 - j0.01 \quad 0.1 - j0.1]^T$ and the step size $\mu = 0.0005$, the learning curves of the LMS algorithm averaged over 20 different runs are plotted in Fig. 5. There were two types of learning curves depicted in Fig. 5, namely, the learning curve realted to the training-based adaptation, when the desired user's transmitted symbol $b_1(k)$ was known to the receiver, and the learning curve related to the decision-directed (DD) adaptation, where at the sample $k = 250$ the beamformer's decision $\hat{b}_1(k)$ was used to substitute for $b_1(k)$. Similarly, the learning curves of the LSER algorithms under the same initial condition of $\hat{\mathbf{w}}(0)$ and given the step size 0.001 and the kernel width $\rho_n = \sigma_n$ are depicted in Fig. 5, in comparison with those of the LMS algorithm. Lastly, the SER performance of both the LMS and LSER based beamformers are compared with those of the theoretic MMSE and MSER solutions in Fig. 6 under the same condition of Fig. 3 (b). The superiority of the adaptive LSER beamformer over the adaptive LMS beamformer is
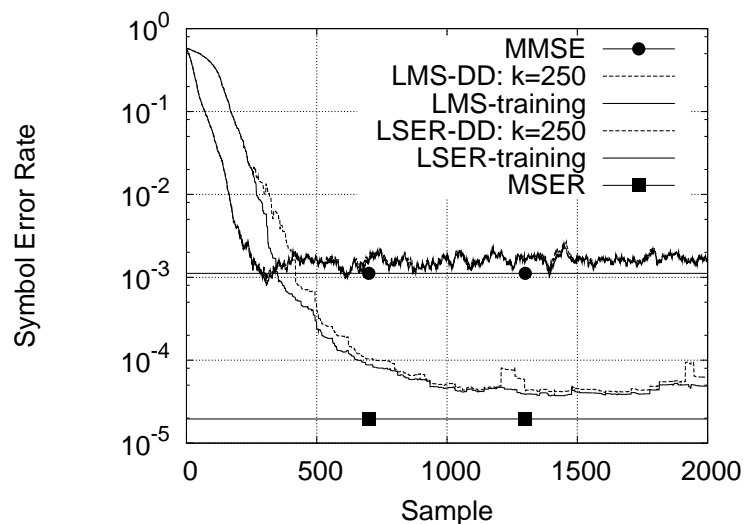

Fig. 5. Learning curves of the stochastic adaptive LMS and LSER algorithms averaged over 20 runs for the non-fading channel system employing the three-element array of Fig. 2 with a minimum angular separation of $\theta = 30°$ to support four equal-power 16-QAM users given SNR= 26 dB, where DD denotes decision-directed adaptation with $\hat{b}_1(k)$ substituting for $b_1(k)$.
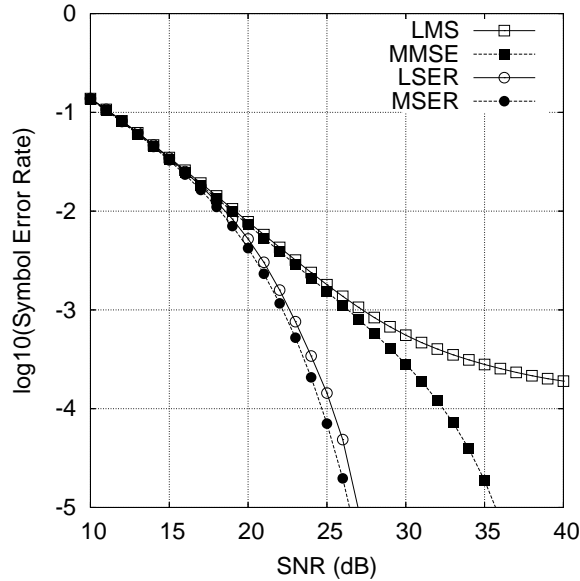
Fig. 6. Desired user's symbol error rate performance comparison for the non-fading channel system employing the three-element array of Fig. 2 with a minimum angular separation of $\theta = 30°$ to support four equal-power 16-QAM users.

clearly demonstrated in Fig. 6, where it can be seen that the performance of the adaptive LMS beamformer was notably deviated from its theoretic MMSE solution at high SNRs.

B. Rayleigh Fading System

The modulation scheme was 64-QAM. Fading channels were simulated, where the magnitudes of A_i for $1 \leq i \leq 4$ were Rayleigh processes with the normalised Doppler frequence $\bar{f}_D$ and each channel A_i had the root mean power of $\sqrt{0.5} + j\sqrt{0.5}$. Thus the average $\text{SIR}_i = 0$ dB for $2 \leq i \leq 4$. Continuously fluctuating fading was used, which provided a different fading magnitude and phase for each transmitted symbol. The transmission frame structure consisted of 50 training symbols followed by 450 data symbols. Decision-directed adaptation was employed during data transmission, in which the adaptive beamforming detector's decision $\hat{b}_1(k)$ was used to substitute for $b_1(k)$. The SER of an adaptive beamforming detector was calculated using the 450 data symbols of the frame based on Monte Carlo simulation averaging over at least 2×10^5 frames, depending on the value of $\bar{f}_D$. Two initialisations were used for the adaptive LMS and LSER algorithms, where the initial weight vector $\hat{\mathbf{w}}(0)$ was initialised to either the MMSE solution (corresponding to the initial channel conditions) or $[0.1 + j0.0 \;\; 0.1 + j0.0 \;\; 0.1 + j0.0]^T$, and the performance were observed to be very similar for these two initialisations.
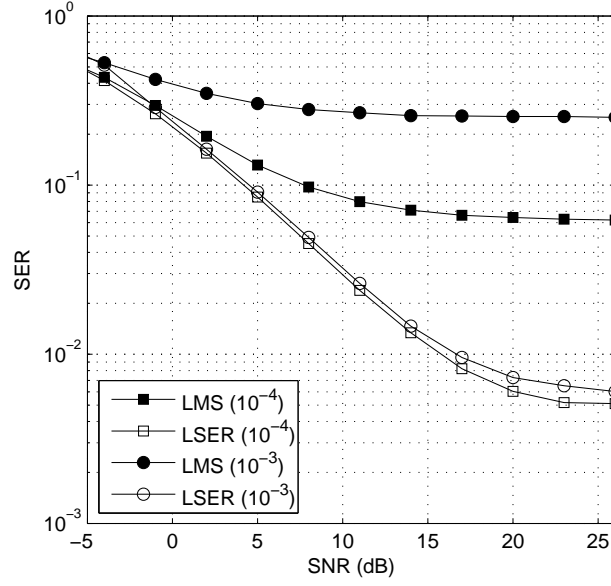
Fig. 7. Desired user's symbol error rate performance comparison for the fading channel systems of the two normalised Doppler frequencies $\bar{f}_D = 10^{-4}$ and 10^{-3} employing the three-element array of Fig. 2 with a minimum angular separation of $\theta = 27°$ to support four 64-QAM users. The LMS algorithm has a step size $\mu = 0.0002$, while the LSER algorithm has a step size $\mu = 0.00005$ and a kernel width $\rho_n = 4\sigma_n$.
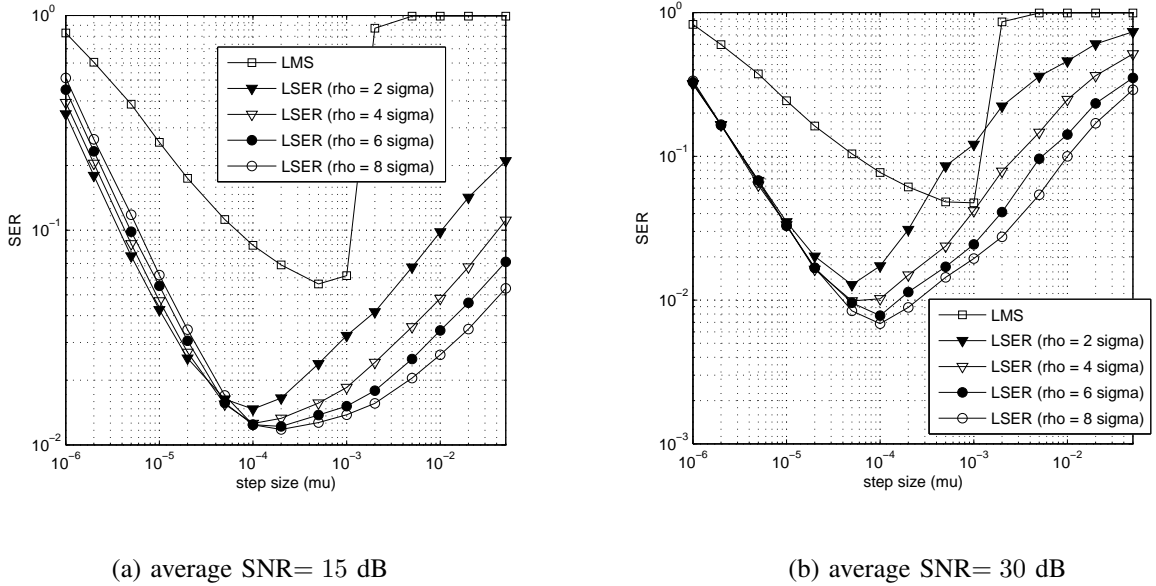

(a) average SNR= 15 dB

(b) average SNR= 30 dB

Fig. 8. Influence of the adaptive algorithm's parameters to the SER performance for the fading channel system employing the three-element array of Fig. 2 to support four 64-QAM users, given $\theta = 27°$ and $\bar{f}_D = 10^{-4}$.

Given the minimum angular separation $\theta = 27°$, Fig. 7 compares the SER of the adaptive LSER beamformer with that of the LMS-based one, for the two normalised Doppler frequencies $\bar{f}_D = 10^{-4}$ and 10^{-3}. It can be seen from Fig. 7 that the SER performance of the adaptive LSER beamformer degraded only slightly when the fading rate increased from $\bar{f}_D = 10^{-4}$ to 10^{-3}. This demonstrates that the LSER algorithm has an excellent tracking ability, capable of operating in fast fading conditions. The influence of the adaptive algorithm's parameters, the step size μ for the LMS algorithm, and the step size μ and kernel width ρ_n for the LSER algorithm, were next investigated. Given $\bar{f}_D = 10^{-4}$, Fig. 8 (a) show the influence of the adaptive algorithm's parameters, μ for the LMS algorithm, and μ and ρ_n for the LSER algorithm, on the SER performance for a low average SNR value of 15 dB (Note that this was a 64-QAM system, and a SNR of 15 dB was relatively low), while Fig. 8 (b) depicts the results for a high average SNR value of 30 dB. These results also explain why $\mu = 0.0002$ for the LMS algorithm and $\mu = 0.00005$ and $\rho_n = 4\sigma_n$ for the LSER algorithm were used in the simulation of Fig. 7.
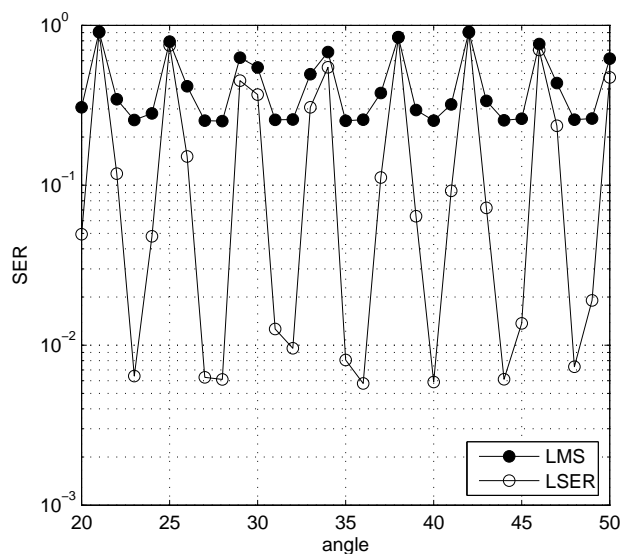

Fig. 9. Desired user's symbol error rate performance as a function of the minimum angular separation θ for the fading channel system of the normalised Doppler frequency $\bar{f}_D = 10^{-3}$ employing the three-element array of Fig. 2 to support four 64-QAM users, given an average SNR of 25 dB. The LMS algorithm has a step size $\mu = 0.0002$, while the LSER algorithm has a step size $\mu = 0.00005$ and a kernel width $\rho_n = 4\sigma_n$.

Lastly, the combining influence of the Rayleigh fading channels A_i, $1 \leq i \leq 4$, and the uniformly varying minimum anugular seapration θ was investigated. Given the normalised Doppler
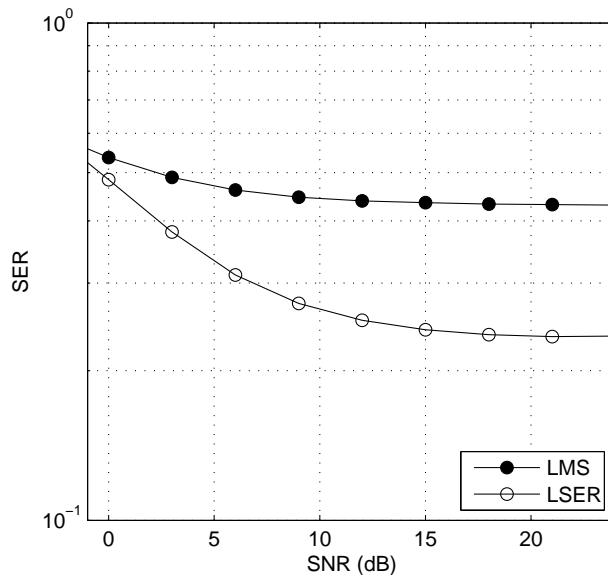
Fig. 10. Desired user's average symbol error rate performance comparison for the fading channel system of the normalised Doppler frequency $\bar{f}_D = 10^{-3}$ employing the three-element array of Fig. 2 with the minimum angular separation θ uniformly distributed in $[20°, \quad 50°]$ to support four 64-QAM users. The LMS algorithm has a step size $\mu = 0.0002$, while the LSER algorithm has a step size $\mu = 0.00005$ and a kernel width $\rho_n = 4\sigma_n$.

frequency $\bar{f}_D = 10^{-3}$ and an average SNR of 25 dB, the minimum angular separation θ was varied in $[20°, \quad 50°]$ and the SER performance of the LMS and LSER adaptive beamformers corresponding to each θ are depicted in Fig. 9. It can be seen from Fig. 9 that the performance of an adaptive beamformer depends on the combination of the channel coefficients A_i, $1 \leq i \leq 4$, and the value of θ, and the adaptive LSER beamformer always performs better than the adaptive LMS beamformer. Finally, the average SER performance of the two adaptive beamformers over the uniformly distributed $\theta \in [20°, \quad 50°]$ are plotted in Fig. 10.

V. CONCLUDING REMARKS

An adaptive MSER beamforming technique has been developed for multiple-antenna aided multiuser communication systems employing high-throughput QAM signalling. It has been demonstrated that the MSER beamforming design can provide significant performance enhancement, in terms of the achievable system's SER, over the standard MMSE design. It has also been demonstrated that the MSER beamforming design offers a higher user capacity and is more robust in the near-far senario, compared with the conventional MMSE beamforming design. An adaptive implementation of the MSER beamforming solution has been realised

using the stochastic gradient adaptive algorithm known as the LSER technique. The simulation results presented in this study clearly show that the adaptive LSER beamforming is capable of operating successfully in fast fading conditions and it consistently outperforms the adaptive LMS beamforming benchmarker.

Since the discovery of turbo codes [45], iterative detection [46] has been applied to joint channel estimation and equalisation [47], multiuser detection [48] and numerous other coded communication systems [49]-[51]. Most of the available literature discuss the MMSE based iterative receivers [49]-[53]. It is however highly desired to consider the MBER based iterative receivers, and the recent work [54],[55] has studied turbo-detected MBER beamformer designs for BPSK and QPSK systems. Currently, the Communication Research Group at the University of Southampton is carrying out extensive investigation to design iterative MSER beamforming detection techniques for employment in the systems that adopt high-order QAM signalling.

The narrow-band MIMO model is considered in this study and beamforming is a spatial only processing technique. In order to deal with the generic frequency-selective MIMO system, space-time processing techniques should be employed. The recent work [56],[57] has designed the novel MBER space-time equalisation for the space-division multiple-access induced MIMO system with BPSK modulation. Extension to the MSER space-time equalisation for the generic MIMO system employing high-throughput QAM modulation schemes is currently being conducted.

REFERENCES

[1] S. Chen, H.-Q. Du and L. Hanzo, "Adaptive minimum symbol error rate beamforming assisted receiver for quadrature amplitude modulation systems," in *Proc. VTC2006-Spring* (Melbourne, Australia), May 7-10, 2006, vol.5, pp.2236–2240.

[2] J.H. Winters, J. Salz and R.D. Gitlin, "The impact of antenna diversity on the capacity of wireless communication systems," *IEEE Trans. Communications*, vol.42, no.2, pp.1740–1751, 1994.

[3] J. Litva and T. K.Y. Lo, *Digital Beamforming in Wireless Communications*. London: Artech House, 1996.

[4] L. C. Godara, "Applications of antenna arrays to mobile communications, Part I: Performance improvement, feasibility, and system considerations," *Proc. IEEE*, vol.85, no.7, pp.1031–1060, 1997.

[5] R. Kohno, "Spatial and temporal communication theory using adaptive antenna array," *IEEE Personal Communications*, vol.5, no.1, pp.28–35, 1998.

[6] J.H. Winters, "Smart antennas for wireless systems," *IEEE Personal Communications*, vol.5, no.1, pp.23–27, 1998.

[7] P. Petrus, R.B. Ertel and J.H. Reed, "Capacity enhancement using adaptive arrays in an AMPS system," *IEEE Trans. Vehicular Technology*, vol.47, no.3, pp.717–727, 1998.

[8] G.V. Tsoulos, "Smart antennas for mobile communication systems: benefits and challenges," *IEE Electronics and Communications J.*, vol.11, no.2, pp.84–94, 1999.

[9] P. Vandenameele, L. van Der Perre and M. Engels, *Space Division Multiple Access for Wireless Local Area Networks*. Boston: Kluwer Academic Publishers, 2001.

[10] J.S. Blogh and L. Hanzo, *Third Generation Systems and Intelligent Wireless Networking – Smart Antenna and Adaptive Modulation*. Chichester, U.K.: John Wiley, 2002.

[11] R.A. Soni, R.M. Buehrer and R.D. Benning, "Intelligent antenna system for cdma2000," *IEEE Signal Processing Magazine*, vol.19, no.4, pp.54–67, July 2002.

[12] A. Paulraj, R. Nabar and D. Gore, *Introduction to Space-Time Wireless Communications*. Cambridge, U.K.: Cambridge University Press, 2003.

[13] A.J. Paulraj, D.A. Gore, R.U. Nabar and H. Bölcskei, "An overview of MIMO communications – A key to gigabit wireless," *Proc. IEEE*, vol.92, no.2, pp.198–218, 2004.

[14] D. Tse, and P. Viswanath, *Fundamentals of Wireless Communication*. Cambridge, U.K.: Cambridge University Press, 2005.

[15] L. Hanzo, S.X. Ng, T. Keller and W. Webb, *Quadrature Amplitude Modulation: From Basics to Adaptive Trellis-Coded, Turbo-Equalised and Space-Time Coded OFDM, CDMA and MC-CDMA Systems*. Chichester, U.K.: John Wiley and IEEE Press, 2004.

[16] I.S. Reed, J.D. Mallett and L.E. Brennan, "Rapid convergence rate in adaptive arrays," *IEEE Trans. Aerospace and Electronic Systems*, vol.AES-10, pp.853–863, 1974.

[17] M.W. Ganz, R.L. Moses and S.L. Wilson, "Convergence of the SMI and the diagonally loaded SMI algorithms with weak interference (adaptive array)," *IEEE Trans. Antennas and Propagation*, vol.38, no.3, pp.394–399, 1990.

[18] B. Widrow, P.E. Mantey, L.J. Griffiths and B.B. Goode, "Adaptive antenna systems," *Proc. IEEE*, vol.55, pp.2143-2159, 1967.

[19] L.J. Griffiths, "A simple adaptive algorithm for real-time processing in antenna arrays," *Proc. IEEE*, vol.57, pp.1696–1704, 1969.

[20] B. Widrow and S.D. Stearns, *Adaptive Signal Processing*. Englewood Cliffs, NJ: Prentice-Hall, 1985.

[21] S. Haykin, *Adaptive Filter Theory*. 3rd edition, Upper Saddle River, NJ: Prentice-Hall, 1996.

[22] S. Chen, L. Hanzo and N.N. Ahmad, "Adaptive minimum bit error rate beamforming assisted receiver for wireless communications," in *Proc. ICASSP 2003* (Hong Kong, China), April 6-10, 2003, vol.IV, pp.640–643.

[23] A. Wolfgang, N.N. Ahmad, S. Chen and L. Hanzo, "Genetic algorithm assisted minimum bit error rate beamforming," in *Proc. VTC 2004-Spring*, May 17-19, 2004, pp.142–146.

[24] I.D.S. Garcia, J.J.S. Marciano, Jr., and R.D. Cajote, "Normalized adaptive minimum bit-error-rate beamformers," in *Proc. IEEE Region 10 TENCON Conf.*, Nov. 21-24, 2004, vol.2, pp.625–628.

[25] Y.-H. Liu and Y.-H. Yang, "Adaptive minimum bit error rate multitarget array algorithm," in *Proc. IEEE 6th CAS Symp. Emerging Technologies: Frontiers of Mobile and Wireless Communication*, 31 May-2 Jun, 2004, vol.2, pp.745–748.

[26] S. Chen, N.N. Ahmad and L. Hanzo, "Adaptive minimum bit error rate beamforming," *IEEE Trans. Wireless Communications*, vol.4, no.2, pp.341–348, 2005.

[27] L.-Y. Fan, H.-B. Zhang and H. Chen, "Minimum bit error rate beamforming for pre-FFT OFDM adaptive antenna array," in *Proc. VTC 2005-Fall*, Sept.25-28, 2005, vol.6, pp.359–363.

[28] N.N. Ahmad, *Minimum Bit Error Ratio Beamforming*, PhD Thesis, School of Electronics and Computer Sciences, University of Southampton, UK, May 2005.

[29] S. Chen, L. Hanzo, N.N. Ahmad and A. Wolfgang, "Adaptive minimum bit error rate beamforming assisted QPSK receiver," in *Proc. ICC 2004*, 2004, vol.6, pp.3389–3393.

[30] S. Chen, L. Hanzo, N.N. Ahmad and A. Wolfgang, "Adaptive minimum bit error rate beamforming assisted receiver for QPSK wireless communication," *Digital Signal Processing*, vol.15, no.6, pp.545–567, 2005.

[31] R. Steele and L. Hanzo, *Mobile Radio Communications*. Piscataway, NJ: IEEE Press, 1999.

[32] S-H. Hwang and L. Hanzo, "Reverse-link performance of synchronous DS-CDMA systems in dispersive Rician multipath fading channels," *IEE Electronics Letters*, vol.39, no.23, pp.1682-1684, 2003.

[33] J.M. Cioffi, G.P. Dudevoir, M.V. Eyuboglu and G.D. Forney, Jr., "MMSE decision-feedback equalizers and coding – Part I: equalization results," *IEEE Trans. Communications*, vol.43, no.10, pp.2582-2594, 1995.

[34] S. Chen, L. Hanzo and B. Mulgrew, "Adaptive minimum symbol-error-rate decision feedback equalization for multi-level pulse-amplitude modulation," *IEEE Trans. Signal Processing*, vol.52, no.7, pp.2092–2101, 2004.

[35] M.S. Bazaraa, H.D. Sherali and C.M. Shetty, *Nonlinear Programming: Theory and Algorithms*. New York: John Wiley, 1993.

[36] S. Chen, A.K. Samingan, B. Mulgrew and L. Hanzo, "Adaptive minimum-BER linear multiuser detection for DS-CDMA signals in multipath channels," *IEEE Trans. Signal Processing*, vol.49, no.6, pp.1240–1247, 2001.

[37] D.E. Goldberg, *Genetic Algorithms in Search, Optimization and Machine Learning*. Reading, MA: Addison Wesley, 1989.

[38] K.F. Man, K.S. Tang and S. Kwong, *Genetic Algorithms: Concepts and Design*. London: Springer-Verlag, 1998.

[39] L. Ingber, "Simulated annealing: practice versus theory," *Mathematical and Computer Modeling*, vol.18, no.11, pp.29–57, 1993.

[40] S. Chen and B.L. Luk, "Adaptive simulated annealing for optimization in signal processing applications," *Signal Processing*, vol.79, no.1, pp.117–128, 1999.

[41] E. Parzen, "On estimation of a probability density function and mode," *The Annals of Mathematical Statistics*, vol.33, pp.1066–1076, 1962.

[42] B.W. Silverman, *Density Estimation*. London: Chapman Hall, 1996.

[43] A.W. Bowman and A. Azzalini, *Applied Smoothing Techniques for Data Analysis*. Oxford, U.K.: Oxford University Press, 1997.

[44] R. Sharma, W.A. Sethares and J.A. Bucklew, "Asymptotic analysis of stochastic gradient-based adaptive filtering algorithms with general cost functions," *IEEE Trans. Signal Processing*, vol.44, no.9, pp.2186–2194, 1996.

[45] C. Berrou and A. Glavieux, "Near optimum error correcting coding and decoding: turbo-codes," *IEEE Trans. Communications*, vol.44, no.10, pp.1261–1271, 1996.

[46] L. Hanzo, T.H. Liew and B.L. Yeap, *Turbo Coding, Turbo Equalisation and Space-Time Coding for Transmission over Fading Channels*. West Sussex, England: John Wiley and IEEE Press, 2002.

[47] L. Hanzo, C.H. Wong and M.S. Yee, *Adaptive Wireless Transceiver: Turbo-Coded, Turbo-Equalised and Space-Time Coded TDMA, CDMA and OFDM Systems*. West Sussex, England: John Wiley and IEEE Press, 2002.

[48] L. Hanzo, L.L. Yang, E.L. Kuan and K. Yen, *Single- and Multi-Carrier DS-CDMA: Multi-User Detection, Space-Time Spreading, Synchronisation, Standards and Networking*. West Sussex, England: John Wiley and IEEE Press, 2003.

[49] X. Wang and H.V. Poor, "Iterative (turbo) soft interference cancellation and decoding for coded CDMA," *IEEE Trans. Communications*, vol.47, no.7, pp.1046–1060, 1999.

[50] M. Tüchler, A.C. Singer and R. Koetter, "Minimum mean squared error equalization using *a priori* information," *IEEE Trans. Signal Processing*, vol.50, no.3, pp.673–682, 2002.

[51] A. Tarable, G. Montorsi and S. Benedetto, "A linear front end for iterative soft interference cancellation and decoding in coded CDMA," *IEEE Trans. Wireless Communications*, vol.4, no.2, pp.507–518, 2005.

[52] M. Tüchler, R. Koetter and A.C. Singer, "Turbo equalization: principle and new results," *IEEE Trans. Communications*, vol.50, no.5, pp.754-767, 2002.

[53] K. Li and X. Wang, "EXIT chart analysis of turbo multiuser detection," *IEEE Trans. Wireless Communications*, vol.4, no.1, pp.300–311, 2005.

[54] S. Tan, L. Xu, S. Chen and L. Hanzo, "Iterative soft interference cancellation aided minimum bit error rate uplink receiver beamforming," in *Proc. VTC2006-Spring* (Melbourne, Australia), May 7-10, 2006, vol.1, pp.17–21.

[55] S. Tan, S. Chen and L. Hanzo, "On multi-user EXIT chart analysis aided turbo-detected MBER beamformer designs," accepted for publication in *IEEE Trans. Wireless Communications*, 2007.

[56] S. Chen, A. Livingstone and L. Hanzo, "Minimum bite-error rate design for space-time equalization-based multiuser detection," *IEEE Trans. Communications*, vol.54, no.5, pp.824–832, 2006.

[57] S. Chen, L. Hanzo, A. Livingstone, "MBER Space-time decision feedback equalization assisted multiuser detection for multiple antenna aided SDMA systems," *IEEE Trans. Signal Processing*, vol.54, no.8, pp.3090–3098, 2006.